[12] G. Mur, "Absorbing boundary conditions for the finite-difference approximation of the time-domain electromagnetic-field equations," *IEEE Trans. Electromagn. Compat.*, vol. EMC-22, pp. 377–382, Nov. 1981.
[13] D. E. Merewether, "Transient currents induced on a metallic body of revolution by an electromagnetic pulse," *IEEE Trans. Electromagn. Compat.*, vol. EMC-13, pp. 41–44, May 1971.
[14] M. Okoniewski, J. Anderson, and S. S. Stuchly, "A technique to compute reflection coefficient in FDTD method," in *IEEE Antennas Propagat. Soc. Int. Symp. Dig.*, Seattle, June 1994, vol. 3, pp. 1446–1449.

Analysis of Anisotropic High Temperature Superconductor Planar Structures on Sapphire Anisotropic Substrates

Mohamed A. Megahed and Samir M. El-Ghazaly

***Abstract*—A full-wave finite-difference time-domain technique is used to study the anisotropy associated with high temperature superconductor (HTS) planar structures. The analysis is performed on anistropic YBCO film deposited on anisotropic sapphire substrate. The solution incorporates all the physical aspects of the HTS materials. The finite thickness of the anisotropic strip is rigorously modeled using a graded non uniform mesh generator. The propagation characteristics of HTS microstrip line are evaluated. The current distributions inside the HTS are calculated for both the normal and the super fluids. It is shown that the 90° r-cut sapphire substrate structure has lower loss and lower effective dielectric constant than the 0° r-cut substrate. Interesting aspects, concerning the anisotropy of HTS microwave structures, are presented.**

I. Introduction

The low surface resistance of superconducting materials is attractive for microwave and millimeter-wave applications such as antennas, filters, delay lines, interconnects, and microwave matching networks. The workhorse HTS materials are $YBa_2Cu_3O_x$, and TlBaCaCuO. They can be deposited on low dielectric loss substrate, such as Silica, Sapphire, Lithium Niobate, MgO, or LaAlO3, to form planar microwave structures. Although the sapphire substrate is anisotropic, the r-cut single crystal sapphire seems to be an appropriate substrate material for HTS applications. To exploit the exciting characteristics of HTS materials, accurate and flexible numerical models have to be developed.

The problem of calculating the propagation characteristics of isotropic superconducting microstrip line has been tackled before using different approaches [1], [2]. However, the field penetration effects is not rigorously modeled in many of those techniques. The finite thickness of the HTS strip need to be taken into consideration, especially when evaluating losses for the propagating wave inside the superconducting microstrip line [3]. Lee *et al.*, presented a full wave analysis that takes into account either the anisotropy in the HTS material or in the substrate itself, based on the spectral domain/volume integral equation approach (SDVIE) [4], [5].

In this paper, we present a technique for modeling a microstrip line incorporating an anisotropic superconducting material deposited on anisotropic sapphire substrate, based on the three-dimensional finite-difference time-domain method. The model incorporates all the physical aspects of the HTS through London's equations. The physical characteristics of the HTS are blended with the electromagnetic model using the phenomenological two fluid model. The complex propagation constant is calculated and the results are compared with the spectral domain technique. The effect of the anisotropy orientation on the characteristics of the microstrip line is studied. Also, effects of the anisotropy on the field distribution inside the structure is studied. This approach fits the needs for accurate computation of the dispersion characteristics of an anisotropic superconducting transmission line.

Manuscript received September 26, 1994; revised April 24, 1995. This work was supported by the National Science Foundation Grant ECS-9108933.

The authors are with the Department of Electrical Engineering, Arizona State University, Tempe, AZ 85287-5706 USA.

IEEE Log Number 9412672.

II. Anisotropic Superconductor Model

The two fluid model assumes that the electron gas in a superconductor material consists of two gases, the superconducting electron gas and the normal electron gas. The main parameters of the superconducting material are the London penetration depth λ_L and the normal conductivity σ_n. The total current density in superconducting material is expressed as follows:

$$\mathbf{J} = \mathbf{J}_n + \mathbf{J}_s \tag{1}$$

where $\mathbf{J}_n$ is the normal state current density. It obeys Ohm's law

$$\mathbf{J}_n = \sigma_n \mathbf{E}. \tag{2}$$

The superconducting fluid current density is obtained using London equation

$$\frac{\partial \mathbf{J}_s}{\partial t} = \frac{1}{\mu_o \lambda_L^2} \mathbf{E}. \tag{3}$$

These expressions are valid assuming that the HTS material is isotropic. However, experiments show that the properties of the HTS materials are anisotropic. Such anisotropy may have significant effects on the device performance. The designer is faced with several choices, such as the type of material and film direction, to obtain the optimum configuration that enhances the characteristics of the HTS material. A common feature of the family of HTS, including YBaCuO and TlBaCaCuO, is that they all have layered crystal structures. It is generally believed that the two-dimensional CuO_2 network is the most essential building block of the HTS materials. Thin-film transmission lines will favor films in which conducting sheets lie in the plane of the film. The anisotropy for the HTS can be represented by an anisotropic conductivity for the normal state, and an anisotropic London penetration depth for the superconducting state. The conductivity tensor $\overline{\sigma}$ is diagonal and is given by

$$\overline{\sigma} = \begin{bmatrix} \sigma_a & 0 & 0 \\ 0 & \sigma_b & 0 \\ 0 & 0 & \sigma_c \end{bmatrix}. \tag{4}$$

Also, the London penetration depth tensor $\overline{\lambda}$ is diagonal, and is written as

$$\overline{\lambda} = \begin{bmatrix} \lambda_a & 0 & 0 \\ 0 & \lambda_b & 0 \\ 0 & 0 & \lambda_c \end{bmatrix} \tag{5}$$

where a, b, and c are the principal axes of the anisotropic superconducting material. The normal conductivity and the London penetration depth in (1)–(3) will be replaced by their corresponding tensors to formulate the anisotropic superconductor model.

Experiments show that for YBCO the HTS parameters along the a- and b-axes are approximately equal. In our discussion, these parameters are the normal fluid conductivity σ_{nab} and the superconducting fluid London penetration depth λ_{ab}. The normal conductivity σ_{nab} equals 10–80 times σ_{nc}, and the penetration depth λ_c equals 3–5 times λ_{ab} [6]. Experiments also report that the critical current density and the upper critical field are anisotropic.

III. Anisotropic Finite-Difference Time-Domain Method

An arbitrary 3-D structures can be embedded in FDTD lattice simply by assigning desired values of electrical permittivity and conductivity to each lattice electric field intensity (**E**) component, and magnetic permeability and equivalent loss to each magnetic field intensity (**H**) component. Specification of the media properties in this component-by-component manner provides a convenient algorithm to represent the anisotropy in a media and assures continuity of tangential fields at the interface of dissimilar media with no need for special field matching.

The FDTD applies central-difference approximations for the space and time derivatives of the electric (**E**) and magnetic (**H**) field intensities directly to the differential operators of the curl equations, when the anisotropy of the material is along its principal axis. The same algorithm can be implemented when the principal axes of the anisotropic material are tilted with respect to the coordinates. In this case, the solution will be carried on the electric (**D**) and magnetic (**B**) flux densities. The algorithm will be extended one step further, to obtain the field intensity using the appropriate constitutive relations. In our discussion, the YBCO HTS strip is assumed to be anisotropic along its principal axis (i.e., c, b, and a along x, y, and z, respectively). The r-cut sapphire substrate is considered for two cases at 0 and 90 degrees rotation about its principal axis (i.e., rotation about x-axis). The configuration simulated in this study corresponds to the practical structure used in [7]. However, the analysis presented here is flexible and can be extended to any anisotropic configuration. The following equation for E_z is obtained by combining Ampere's law with the two fluid model

$$\frac{\partial E_z}{\partial t} = \frac{1}{\varepsilon}\left(\frac{\partial H_y}{\partial x} - \frac{\partial H_x}{\partial y} - \sigma E_z - J_{sz}\right) \tag{6}$$

where the superconducting current density J_{sz} is obtained from (3). The other field components are similarly obtained. It is known that the physical parameters of the different materials are defined at each point in the FDTD approach.

The developed three-dimensional finite-difference time-domain scheme is capable of modeling the finite thickness of the HTS strip. No approximations are made to the strip thickness. A graded nonuniform mesh generator is used to dicsretize the simulation domain, where the smallest mesh size is chosen inside and around the HTS strip [3]. The ground plane is chosen as a perfect electric wall, for simplicity. The symmetry of the structure is used, and the simulation is carried only on half the structure. The computation domain is closed by absorbing boundary conditions. The Courant stability condition is based on the smallest mesh step size. A Gaussian pulse excitation is used at the front surface. The tangential magnetic field is assumed to have only the H_y component. The smallest wavelength existing in the computational domain is chosen to be greater than 40 the maximum mesh step size to reduce the truncation and the grid dispersion errors in nonuniform mesh discretization scheme. Once the temporal fields are obtained, the effective dielectric constant and the attenuation constant can be calculated from the discrete Fourier transform of these fields. The computer code for our analysis is written in FORTRAN 90 and is executed in massively parallel machine (MASPAR) environment.

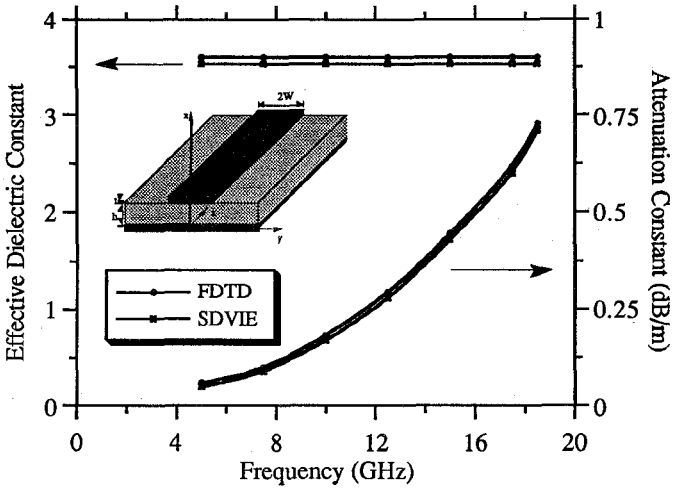

Fig. 1. The propagation characteristics of anisotropic HTS on isotropic substrate using the anisotropic FDTD and SDVIE.

IV. Results and Discussions

A microstrip line with YBCO HTS material on a sapphire substrate, as shown in Fig. 1, is analyzed using the previously described technique. The HTS strip has penetration depth $\lambda(0K) = 0.14\,\mu$m, normal conductivity $\sigma_n(T_c) = 2.08 \times 10^6$ S/m, and critical temperature $T_c = 92.5$ K. The frequency independent penetration depth and the normal conductivity equal to 0.2 μm and 1.0×10^6 S/m, respectively, at 77 K. The dimensions of the microstrip line are as follows: strip width $2W = 2\,\mu$m, substrate height $h = 1\,\mu$m, and HTS strip thickness $t = 0.5\,\mu$m. These dimensions are selected to allow comparing our results with those presented by Lee *et al.* [4].

The simulation is performed for a microstrip line with isotropic substrate with dielectric constant $\varepsilon_r = 3.9$. Two cases of the HTS strip are considered, the isotropic and anisotropic HTS. The anisotropic characteristics of the HTS are presented by anisotropic penetration depth, $\lambda_c = 5\lambda_{ab}$, and anisotropic normal conductivity, $\sigma_{nab} = 50\sigma_{nc}$ [6]. The principal axes of the HTS film is aligned with the coordinate axes. The c-axis is assumed to be in the x-direction. The results calculated for the effective dielectric constant and attenuation constant, for both the isotropic and anisotropic HTS strip on isotropic substrate are shown in Fig. 1. These results are also compared with those obtained by Lee *et al.* [4] using the SD/VIE approach. Our results are in good agreement with the previously published ones. A slight increase in the effective dielectric constant accompanied by a small increase in the attenuation constant is observed in Fig. 1. Obviously, this slight change is due the larger field penetration in the FDTD treatment compared to the SDVIE approach and the way the current distribution is represented in both methods. This clearly demonstrates the accuracy and the consistency of our model. The effect of the HTS anisotropy, on the propagation characteristics of the microstrip line, is negligible due to the orientation of the thin film HTS strip. The HTS anisotropy is in the x-direction where the currents is very small in a microstrip line structure. The distribution of the normalized longitudinal current density component (J_z) at the bottom surface of the HTS strip for the normal and the super gases are shown in Fig. 2. The values and the distributions are approximately equal for both cases, isotropic and anisotropic HTS strip. This can explain the similarity in the effective dielectric constant and the attenuation constant for both cases, isotropic and anisotropic HTS films.

The study of the anisotropy is carried on an anisotropic HTS strip on sapphire anisotropic substrate. The anisotropic YBCO HTS strip

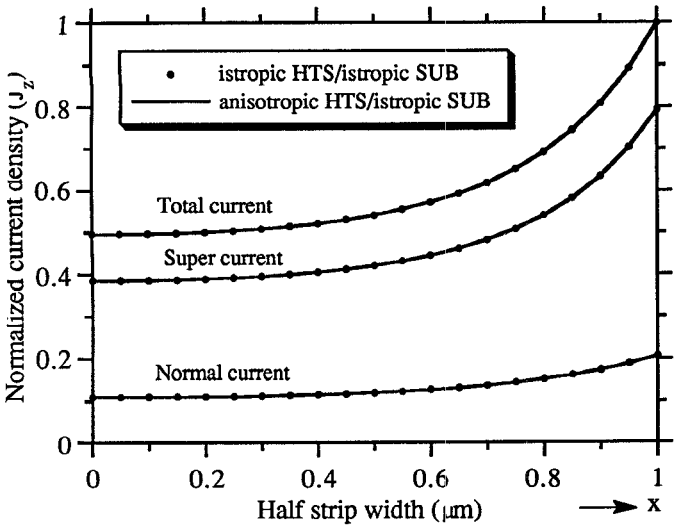

Fig. 2. Normalized normal-fluid, super-fluid, and total current densities at the bottom surface of the strip, for both the isotropic and anisotropic HTS cases, on isotropic substrate.

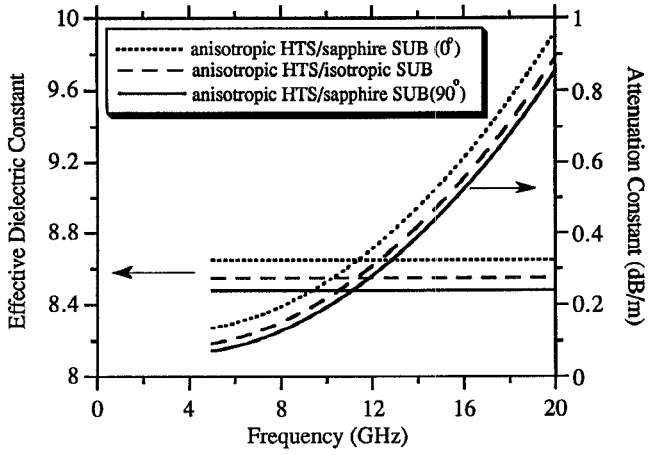

Fig. 3. The propagation characteristics for anisotropic HTS on different r-cut anisotropic sapphire substrates and on isotropic substrate with ε_r =10.03.

has the same characteristics as before. Anisotropic microstrip line with the same dimensions as presented above is used in this study. The anisotropy of the sapphire substrate is represented by the dielectric permittivity tensor. For the 0° r-cut sapphire, the relative permittivity tensor is ε_{xx} =10.03, ε_{yy} =10.97, and ε_{zz} =9.4 along x, y, and z directions, respectively. The tensor is ε_{xx} =10.03, ε_{yy} =9.4 and ε_{zz} = 10.97 for the 90° r-cut [7]. The angle is calculated with respect to the rotation about the x-axis. To assess the effect of the substrate anisotropy, a comparison will be made between the performance of the microstrip line on a sapphire substrate with a similar structure on an isotropic substrate with a relative permittivity ε_r =10.03. It should be noted that the chosen relative dielectric constant of the isotropic substrate equals to the element of the anisotropic dielectric tensor ε_{xx}. In the microstrip line configuration, the electric field in the x-direction is the strongest, thus the propagating wave velocity strongly depends on the value of the relative permittivity in that direction.

Fig. 3 shows the attenuation constant for the anistropic HTS on r-cut sapphire substrate as a function of the rotation angle about the x-axis at two different angles, 0° and 90° and for anistropic HTS on isotropic substrate with ε_r =10.03. The microstrip line on anisotropic sapphire substrate with 0° r-cut has the highest attenuation. The 90° r-cut produces the lowest attenuation of the three structures. The

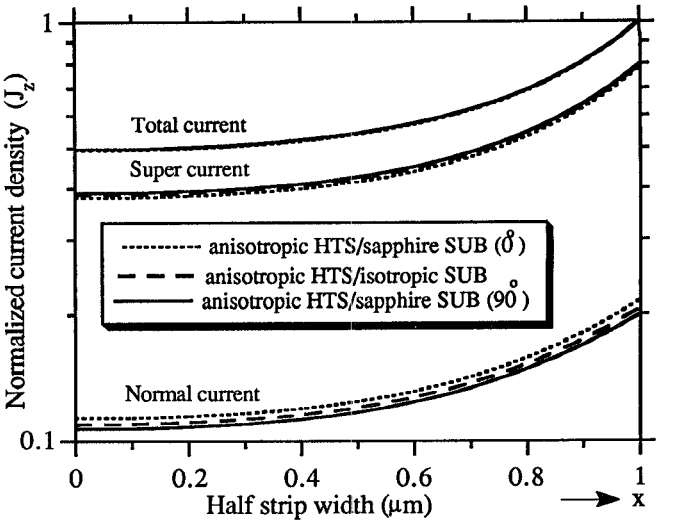

Fig. 4. The normal-fluid, superconducting-fluid, and total current densities for anisotropic HTS on different r-cut sapphire substrates and on isotropic substrate with ε_r =10.03.

effective dielectric constants ε_{reff} of the three structures are also depicted in Fig. 3. The 0° r-cut sapphire substrate results in the highest ε_{reff}, while the 90° r-cut substrate produces the lowest. The change in the propagation characteristics can be explained by the value of the permittivity tensor element ε_{yy} in the y-direction. The y-field component of the fringing field increases with the increase of ε_{yy} from 9.4 (90° rotation) to 10.03 (isotropic) to 10.97 (0° rotation), which in turn increases the energy stored in the substrate and results in the decrease of the propagating wave velocity on the line or increase in the effective dielectric constant. The increase in the attenuation constant can be explained by considering the various current distributions presented in Fig. 4. It is shown that the normal current density is the largest for the 0° r-cut and it is the lowest for the 90° r-cut substrate. This explains the slightly higher attenuation in the 0° r-cut case.

V. Conclusion

A full-wave analysis for anisotropic HTS planar microwave structures deposited on anisotropic substrates is presented. The FDTD technique, which takes the finite thickness of the anisotropic HTS film into consideration, is developed using a graded non uniform mesh generator. This procedure is general, rigorous, and yet flexible. It can be applied to any HTS planar microwave structure. The propagation characteristics of the anisotropic HTS microstrip line on r-cut sapphire substrate are calculated as function of different angles with respect to the propagating direction. It is shown that the 90° r-cut sapphire substrate structure has lower loss and lower effective dielectric constant than the 0° r-cut one. These observations are explained by the current distributions on the HTS strip. The 0° r-cut substrate results in higher losses, which is consistent with the high effective dielectric constant for this cut. The approach presented can be used not only to obtain the characteristics of HTS microwave structures but also to determine the optimum design that exploits the HTS characteristics on anisotropic substrates.

References

[1] J. M. Pond, C. M. Krowne, and W. L. Carter, "On the application of complex resistive boundary conditions to model transmission lines consisting of very thin superconductors," *IEEE Trans. Microwave Theory Tech.*, vol. 37, pp. 181–189, 1989.

[2] H. Lee and T. Itoh, "Phenomenological loss equivalence method for planar quasi-TEM transmission lines with a thin normal conductor or

superconductor," *IEEE Trans. Microwave Theory Tech.*, vol. 37, pp. 1904–1909, 1989.
[3] M. A. Megahed and S. A. El-Ghazaly, "Finite difference approach for rigorous full-wave analysis of superconducting microwave structures," in *IEEE MTT-S Int. Microwave Symp. Dig.*, June 1993.
[4] L. Lee, S. Ali, and W. Lyons, "Full-wave characterization of high-Tc superconducting transmission lines," *IEEE Trans. Appl. Superconduct.*, vol. 2, no. 9, pp. 49–57, 1992.
[5] L. Lee, W. Lyons, T. Orlando, S. Ali, and R. Withers, "Full-wave analysis of superconducting microstrip lines on anisotropic substrates using equivalent surface impedance approach," *IEEE Trans. Microwave Theory Tech.*, vol. 41, no. 12, pp. 2359–2367, 1993.
[6] Y. Iye, *Studies of High Temperature Superconductors: Anisotropic Superconducting and Normal State Transport Properties of HTSC Single Crystals.* New York: Nova, 1989.
[7] I. B. Vendik *et al.*, "CAD model for microstrips on r-cut sapphire substrates," submitted to *Int. J. Microwave and Millimeter-Wave Computer-Aided Engineering*, 1994.

Quasi-TEM Analysis of V-Shaped Conductor-Backed Coplanar Waveguide

Kwok-Keung M. Cheng and Ian D. Robertson

***Abstract*—In this paper, a new type of V-shaped conductor-backed coplanar waveguide (VGCPW) is proposed. The characteristic impedance of the new line is obtained analytically using conformal mapping method under the assumption of pure-TEM propagation and zero dispersion. Direct solutions for the quasistatic normal electric field components and cumulative electric flux distribution across conductor surfaces are also presented. The numerical results show how the total electric flux terminating on the conductor surfaces varies in terms of the CPW's geometry and substrate parameters.**

I. Introduction

A thin-dielectric microstrip was recently introduced by ATR in Japan as a highly miniaturized microstrip medium for MMIC's [2]. In this technique, a ground-plane is deposited on top of the semiconductor substrate and miniature microstrip lines are then realized with very narrow tracks on top of a thin polyimide or silicon oxynitride dielectric film. Typically, 50-Ω lines are less than 10 μm wide, compared to 140 μm for conventional microstrips. However, the losses in these very narrow conductors are very high because of current crowding near the conductor edges. For these reasons, ATR's have more recently demonstrated a "valley microstrip," in which the conductor cross-section is made V-shaped in order to make the current distribution more uniform and reduce the losses [3], [4]. In this paper, a new type of coplanar waveguide structure is proposed. This line may be considered as an evolution of the conventional coplanar structure [1], where the geometry of the transmission line is essentially a conductor-backed CPW in which the lower ground plane is bent within the dielectric in a V-shape to form the equal sides of an isosceles triangle [see Fig. 1(a)]. The angle between the two ground sides is the parameter 2β. The distance between the strip conductor and the center of the valley ground plane is d. The bending of the ground plane into a triangle shape is a major deviation from the standard coplanar structure since the field configuration is significantly modified. This new structure can reduce the current concentration at both edges of the strip conductor, since the distance between the center of the valley ground plane and the strip conductor is smaller than between the valley ground plane and the edge of the strip conductor. The concentration of current is therefore dispersed between three points, i.e., the center and both edges of the center conductor. The quasi-TEM characteristic properties of the new structure to be studied is obtained by the conformal mapping method.

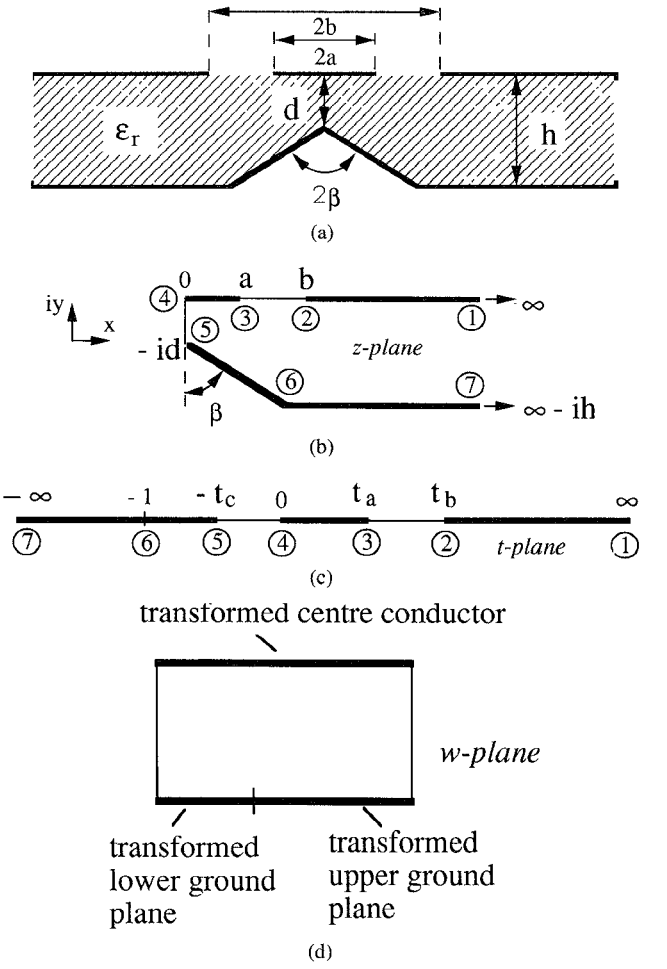

Fig. 1. Conformal mapping of VGCPW.

II. V-Shaped Conductor-Backed CPW

The new type of CPW configuration under analysis is shown in Fig. 1(a), where the ground planes are assumed to be sufficiently wide as to be considered infinite in the analytical model. All metallic conductors are assumed to be infinitely thin and perfectly conducting. The central conductor, of width $2a$, is placed between the two upper ground planes, of spacing $2b$, which are located on a substrate of thickness h, with relative permittivity ε_r. It is assumed that the air-dielectric boundary between the center conductor and the upper ground plane behaves like a perfect magnetic wall. This ensures that

Manuscript received November 14, 1994; revised April 24, 1995. This work was supported by the Engineering and Physical Sciences Research Council (EPSRC), U.K.

The authors are with the Communication Research Group, Department of Electronic & Electrical Engineering, King's College London, University of London, Strand, London, England WC2R 2LS.

IEEE Log Number 9412671.